GEOPHYSICAL RESEARCH LETTERS, VOL. 23, NO. 16, PAGES 2161-2164, AUGUST 1, 1996

Molecular excitation in Sprites

B.D. Green, M.E. Fraser, W.T. Rawlins, L. Jeong, W.A.M. Blumberg, S.B. Mende,
G.R. Swenson, D.L. Hampton, E.M. Wescott, and D.D. Sentman

Abstract. We have determined the molecular internal energy distribution in the N_2 $B^3\Pi_g$ state from the fluorescence measured during the observations of sprites during 1995. Spectrally resolved data from two different instruments and three different sprites are compared with theoretical spectra to obtain excited state vibrational distributions. Energy dependent electron excitation cross-sections and laboratory data were used to estimate the energies of electrons producing the red sprite radiance. Implications for chemical production in the mesosphere and critical future measurements are discussed.

Introduction

Red sprites and blue jets are middle-atmospheric electric discharges linked to lightning. Sprites have been reported episodically for many years, but systematic investigation has begun only recently [Lyons, 1994; Sentman & Wescott, 1993; Sentman et al., 1996]. We present an analysis of the spectral data from observations of the visually red portion of the sprite column at altitudes near 70 km. Two groups have reported spectra obtained from ground based instruments. Hampton et al. [1996] used a TV slit spectrograph with the slit positioned horizontally so that emission from a single altitude was observed. Sprites were observed from Mt. Evans, CO in June 1995 with this instrument operated at two different spectral resolutions. Mende et al. [1995] used a bore sighted intensified CCD video system with a slit and transmission grating positioned vertically observing from Yucca Ridge, CO in July 1995. Details of these instruments and observations are contained in their respective papers. Both groups identified emissions from N_2 First Positive ($B^3\Pi_g \rightarrow A\ ^3\Sigma_u^+$) as the only significant emission within their instrumental bandpass. Vibrational levels in the B-state up to at least v=6 [Mende et al. (1995)] and 10 [Hampton et al. (1995)] were identified.

We present a spectral analysis to extract upper-state vibrational distributions from the observational data. Energy-dependent electron excitation cross-sections for N_2 electronic states were used to bound the electron energy distribution responsible for the excited-state vibrational populations. This stratospheric/mesospheric discharge process appears to be highly variable. The analysis below draws conclusions based on the first spectral data of the red sprite column. Insight and spectra of the other facets of sprites await future measurement campaigns.

Spectral Analysis

We have presented details of our spectral analysis code previously (Fraser et al., 1988) as applied to extract detailed excitation mechanisms in the aurorally disturbed upper atmosphere and in chemical flow reactors. The line strengths and positions for all transitions in the $N_2(B^3\Pi_g\text{-}A^3\Sigma_u^+)$ (1PG) for v'=2-12 and $N_2^+(A^2\Pi_u\text{-}X^2\Sigma_g^+)$ (Meinel) for v'=2-5 were included in the comparisons. The spectral fitting technique was employed first to determine the actual spectral resolutions and then to determine the presence and vibrational extent of the nitrogen 1PG and Meinel emissions. The Mende et al.[1995] data were best reproduced with a triangular slit function of 5 nm resolution. The Hampton et al. [1996] high and low resolution data were best reproduced with slit functions of 2 and 6 nm.

The molecular rotational levels were modeled to be in thermal equilibrium at a temperature of 220 K. The spectral resolution in the data does not permit accurate rotational temperature determination. Fits with temperatures as high as 300 K were also consistent with the data. The theoretical spectra were calculated at high resolution, and then convolved with the slit function. Although the data from both instruments was spectrally response corrected, atmospheric attenuation by the O_2 (b-X) system around 762 nm, and the rapid decrease in detector response beyond 750 nm, make the 1PG $\Delta v=2$ and Meinel $\Delta v=2$ sequence data in this region less accurate.

The experimental data were corrected for atmospheric transmittance using MODTRAN predictions [Anderson et al., 1993]. The transmittance was calculated assuming a 400 km atmospheric path length from a 10,000 ft ground point to 45 and 85 km altitudes. The resulting transmittance data were convolved with a slit of equivalent resolution and applied to the experimental data. Because atmospheric absorption of the N_2 1PG transitions occurs over Voigt lineshapes, this treatment is not exact. However, because the atmospheric column density profiles in the wake of the thunderstorm are not accurately known, a more exact treatment was not warranted in this analysis. The effects of errors in the instrumental radiance response were minimized by determining the vibrational populations in each spectral sequence separately.

The population in each vibrational level is not set by a "temperature" but rather determined by the linear solution vector that minimizes the least-squares difference between the computed and observed spectra. To achieve spectral alignment, the data from both instruments had to be spectrally shifted by less than the resolution to best match the theoretical spectra. The spectrum of a red sprite at 2 nm resolution (Hampton et al. [1996]) is presented in Figure 1a. The sprite emission originates from an altitude estimated to be about 70 km [Sentman et al., 1996]. The synthetic spectrum resulting from the best fit to the data is also shown. Both N_2(B-A) and N_2^+(A-X) transitions are included in the theoretical spectrum, however, only 1PG features up to v'=8 are definitely observed. Meinel emission from v'=2 would be most prominent at 780 nm, v'=3 at 810 nm, and v'=4 at 700 nm. The observed radiance in these regions is at the noise level, thus N_2^+(A) populations can only be set as upper bounds. The derived populations are plotted in Figure 2 as the AK-HI points. The

Paper number 96GL02071
0094-8534/96/96GL-02071$05.00

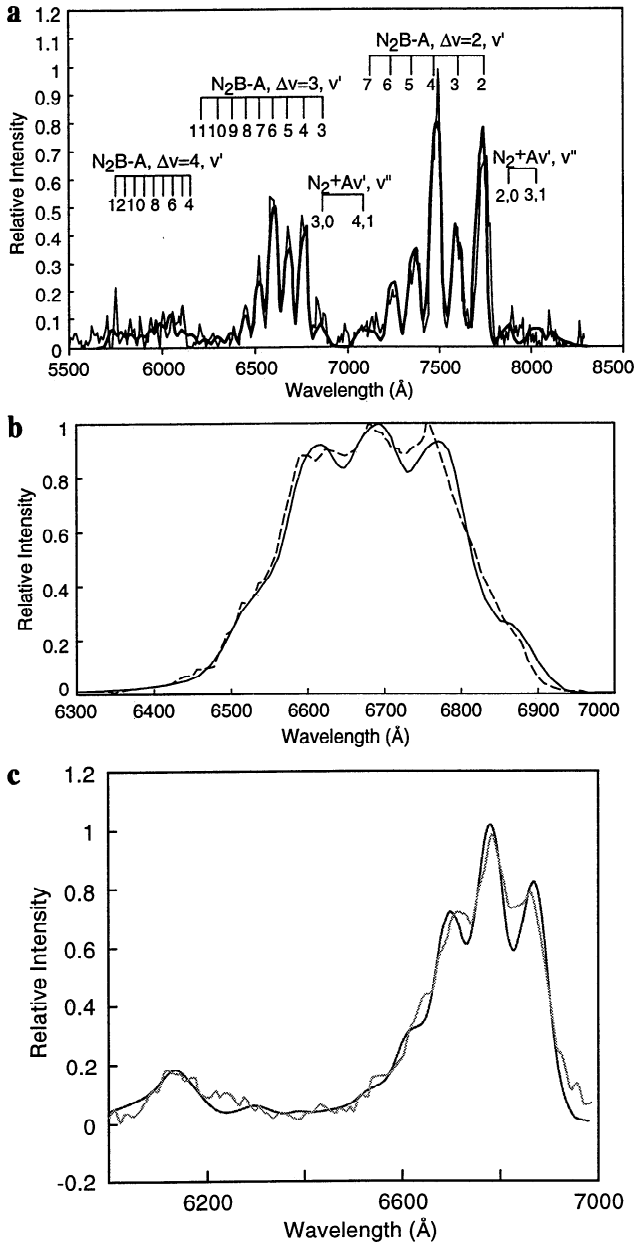

Figure 1. Comparison of synthetic spectra of N_2 B-A and N_2^+ A-X emissions (bold, smoother lines) with response corrected spectra from sprites (lighter/broken lines). Features are labeled in Figure 1A. (a) Hampton et al. at 2 nm res. (AK-HI); (b) Hampton et al. at 6 nm res. (AK-LO); (c) Mende et al. at 5 nm res. (MENDE).

uncertainties for B,v=9-11 as indicated are ±0.0012 based on the fitting errors and noise levels.

The lower resolution (6 nm) spectrum of a different sprite by Hampton et al. [1995] is presented in Figure 1b. A dramatic improvement in signal to noise ratio results at this decreased resolution, permitting more detailed analysis. N_2(B) vibrational levels up to v=11 are present above the noise level. The Meinel transitions are not detectable above the noise level. An upper bound on their population is based on the small noise levels present in the spectrum. The populations determined from fitting are presented as the points labeled AK-LO in Figure 2.

The spectrum obtained by Mende et al.(1995) is presented in Figure 1c. It contains emission from a range of altitudes, but emission from about 70 km is felt to dominate. Although this spectrum has greater noise than the data of Figures 1a and 1b, a good comparison to the theoretical spectrum is obtained. The calculated distribution decreases more rapidly with v. This may be due to inexact baseline correction, variability between different sprites, or the inclusion of emission from lower altitudes by the vertical slit orientation. N_2(B) $v \leq 8$ are present above the noise level. Vibrational populations derived from the three sprite spectra are plotted in Figure 2.

At these altitudes, collisional quenching competes with radiative decay from the allowed electronic transitions. Consequently, comparison of sprite data to other atmospheric emissions, such as observed during auroral events at higher altitudes, is not straightforward. The Meinel transitions will be severely quenched [Piper et al., 1985]. Comparison with laboratory data acquired in electron irradiated nitrogen and air mixtures at pressures representative of 70 km altitudes permits the vibrational distributions and ion/neutral relative populations to be compared against expectations based on electron excitation cross-sections and molecular quenching. These data were acquired with the LABCEDE Facility at the Phillips Lab Geophysics Directorate [Green et al., 1988]. A monoenergetic beam of 4 keV electrons was introduced into a 0.9 m diameter chamber containing a well-mixed nitrogen/oxygen gas mixture.

The N_2 B-state and N_2^+ A-state vibrational distributions from collisional quenching of N_2^* produced by keV energy electron excitation as measured in this facility at pressures corresponding to 70 km altitudes is also shown in Figure 2. Levels B, v=8-10 are produced more abundantly by keV electrons than in the sprite distributions. Laboratory N_2^+ A-state populations are comparable to the upper bounds of the Mende and Hampton high resolution data. However, the lab data are significantly greater than the N_2^+A population bounds on the Hampton et al. low resolution data. Future campaigns should target accurate measurement of the Meinel bands as a critical indicator of the electron energy causing the excitation.

The relative B-state populations in levels 2,4-7 are similar in all three sprite observations and the laboratory data. The (3-0) feature is relatively weak and dominated by the experimental noise level. The (3-1) transition is severely attenuated in the atmospheric path. Incomplete correction for this attenuation results in an inexact determination of the v'=3 population.

The higher B-state levels have the smallest radiances. To minimize the contribution from noise, we subtracted a baseline from the data. The populations for $v' \geq 9$ are most significantly affected. The low resolution data from Hampton et al. [1995] has the best signal levels, exhibits a monotonic decrease with increasing v, and provides the most accurate high v population determination. Emission from states up to v'=11 is observed.

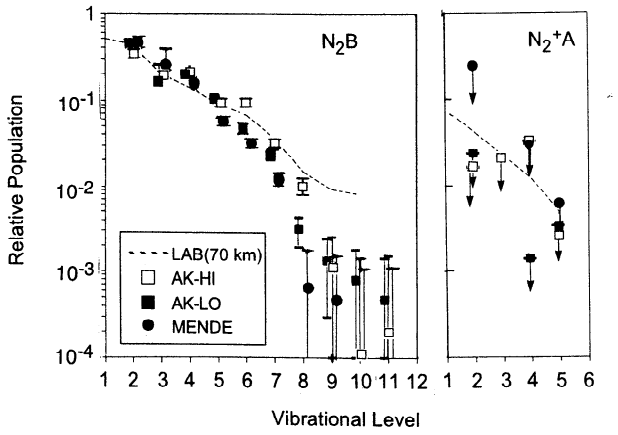

Figure 2. Vibrational distributions deduced from Figure 1 and laboratory observations (---); AK-HI (*); AK-LO (■); MENDE (●). Baseline subtraction applied.

This state lies at an energy near the dissociation limit for nitrogen, and only a few eV below the ionization threshold. Atoms and ions created in the sprite may act as precursors to initiate chemical reactions affecting the atmospheric odd nitrogen (NO) and oxygen (O,O_3) budgets.

To provide further insight, we undertook simple modeling of the electron-impact excitation processes that could produce the observed sprite distributions. The excitation cross sections of each vibrational level in the N_2 B and C and N_2^+ A states as a function of energy have been measured by Stanton and St. John [1969]. The excitation spectrum is quite structured, peaking in the 10 eV region for low v′ and increasing with v′. Cascade from the C-state peaks for 14 eV electrons and is a significant contribution to the total B-state excitation for the lower levels. We calculated the excitation of each vibrational level in each electronic state for all electron energies between 6 and 100 eV at 0.25 eV intervals. The distribution in the B-state changes significantly for electron energies in the 8 to 14 eV range. Ion A-state emission is a sensitive indicator of the presence of high energy electrons, with a peak in the excitation cross-section near 100 eV and a threshold above 15 eV.

At 70 km altitudes both the B- and ionic A-states are quenched. Using measured lifetimes [Piper et al., 1989] and quenching rate coefficients for the B-state [Piper et al.,1992] and the A-state [Piper et al., 1985], the expected radiance levels and vibrational distributions at 70 km altitude were modeled as a function of electron energy. Quenching of the A-state is severe with only 5 to 7% of the excitation escaping as fluorescence. The ionic B-state (with prominent emissions at 391.4 and 427.8 nm) is less sensitive to quenching, but is severely attenuated due to atmospheric scattering. MODTRAN calculations showed this attenuation to be one to two orders of magnitude at 427.8 nm, being a very sensitive function of aerosol loading and look angle. Intensities of tens of kR of 427.8 nm emission from red sprites have been observed using a ground-based radiometer [Armstrong, 1995].

The observations are compared to predictions based on both mono-energetic electron excitation, and electrons with a Boltzmann approximation for the distribution of energies. Mono-energetic electrons at 100 eV match the shape of both B and ion A-state distributions observed in LABCEDE. The LABCEDE ion A-state populations are higher as expected for the higher energy 4 keV source [Green et al., 1988].

The energies of electrons producing the sprites can be bounded through model comparison with the deduced B- and ion A-state populations. The derived population distribution based on the low resolution spectrum from Hampton et al. [1995] is shown in Figure 3 in comparison with the predicted distributions for several characteristic Boltzmann electron temperatures. The B-state distribution is best matched using a 1 eV Boltzmann electron distribution. A Druyvesteyn distribution with a suppressed high-energy tail may be more realistic. Thus 1 eV represents a lower bound to the characteristic electron temperature. The mono-energetic predictions reveal that electrons with energies above 9.25 eV must be present to excite $N_2(B,v'\geq 8)$. The population distributions from the Mende et al. data and the Hampton et al. high resolution data agree best with Boltzmann electron temperatures of 0.4 and 2 eV respectively, and require mono-energetic electrons of 8.8 and 9.5 eV to be present. These differences appear to be statistically significant and may represent variability in the electron distributions producing these different sprites.

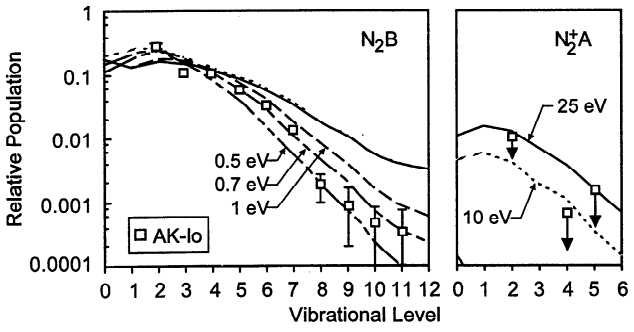

Figure 3. Populations derived from AK-LO data compared with population distribution produced by Boltzmann electron temperature of 0.5, 0.7, 1, 10 , and 25 eV.

The ion A-state populations are not well determined by this analysis. The data points represent upper bounds. The values as plotted indicate that a Boltzmann electron distribution of 10 to 25 eV would be required to produce the populations at the upper bound levels. Electrons above these energies cannot be present at any significant concentration. The B-state provides a more accurate estimation of the electron energy distribution. We cannot distinguish the effects of noise levels in the individual spectra from true variability of the sprite phenomena with such a sparse data set. The population distributions and electron energies may vary for different sprite events.

The implications of these distributions can be addressed through numerical solutions of the Boltzmann transport equation, that incorporates detailed inelastic energy transfer cross-sections to solve for the electron energy distribution as a function of the parameter E/N. E/N is the ratio of the electric field per unit length to the total number density. Convolution of the electron energy distributions with species excitation cross-sections gives rate coefficients for the key excitation processes as functions of E/N. The electron energy distributions that match the sprite distributions suggest E/N on the order of 10^{-15} V cm^2 and 100 to 200 V/m electric fields at 70 km. Qualitative comparison to spectra observed in laboratory microwave discharges for E/N spanning the (0.9 to 20) x 10^{-15} V cm^2 range [L.G. Piper, private communication] lead to similar conclusions. These values are consistent with theoretical predictions based on lightning-induced electromagnetic pulses (Milikh et al, 1995) and heating by quasi-electrostatic thundercloud fields (Pasko et al, 1995), but not with values required for runaway electron mechanisms (Chang and Price, 1995). However, the absence of obvious $N_2^+(A\rightarrow X)$ transitions in sprite spectra does not by itself preclude E/N values in excess of the runaway electron threshold. Our excitation modeling of N_2^+ B-state production indicates that atmospheric regions having (order of 10^{-15} V cm^2) could produce ionization and tens of kR radiances as observed by Armstrong et al. [1995].

Low-energy discharges of this type generate sufficient electronic excitation, dissociation, and ionization to initiate atomic and excited-state chemical reactions such as the formation of NO, N_2O, and O_3, perturbing the local photochemical balances of odd-nitrogen and odd-oxygen in the stratosphere and mesosphere. A simple mechanism (based on Rawlins et al., 1989) for sprite-induced NO production near 70 km is electron dissociation of N_2 followed by atomic excitation to $N(^2D, ^2P)$, followed by reaction with O_2 to form NO. The dissociation and excitation rate coefficients are strongly dependent on E/N (through their sensitivities to the electron energy distribution). For the conditions of 2 x 10^{-15} Volt cm^2 and 10^3 electrons/cm^3, the local NO production rate for a 10 ms sprite at 70 km is $\approx 10^2$ molecules cm^{-3}s^{-1}, which is comparable to the background photochemical NO production rate. However, this rate is extremely sensitive to E/N and to the square of the sprite's

electron number density, resulting in many orders of magnitude uncertainty. For fixed electron number density, the computed NO production rate increases almost two orders of magnitude upon doubling E/N, and decreases by over three orders of magnitude upon halving E/N. Thus factor of two uncertainty in E/N encompasses 5 to 6 orders of magnitude in the local NO production rate. Discharge intensities, durations, and frequency of occurrence are highly variable, further complicating assessment of local and regional chemical production rates. Clearly, reliable estimates of E/N for a large range of sprite-related phenomena and altitudes are required to evaluate their atmospheric chemical impacts. This can be accomplished through analysis of emission spectra giving neutral and ionic excited-state population distributions as demonstrated here. If NO production is indeed significant, it may be possible to observe infrared fluorescence from NO(v). Atmospheric aerosol and molecular scattering are reduced in the infrared spectral region, possibly permitting observation of NO(v) and N_2^* emissions that will provide increased insight into the sprite electron excitation energies and mechanisms.

Conclusions

Spectrally resolved emissions from different sprites taken by two different instruments have been analyzed to extract the transient vibrational distributions resulting from the excitation process(es). Nitrogen First Positive (B-A) transitions dominated all the observations in this wavelength range. While low signal levels and atmospheric transmission compromise the accuracy of the data and analysis, spectral fitting permitted accurate excited state population determination. The relative B-state populations in levels 2,4-7 are similar in all three sprite observations. The low resolution spectrum from Hampton et al. (1996) has the best signal levels, and exhibits a distribution monotonically decreasing with increasing v. The distributions are consistent with excitation by electrons with a Boltzmann temperature of 1 eV (range 0.4 to 2 eV). The variations may be due to different electron distributions present in the different sprite observations.

The sprite electrons appear to be of energy sufficient to dissociate and ionize N_2. The magnitude of this dissociation and ionization and its effect on stratospheric and mesospheric odd-N and odd-O budgets remain key unknowns. There is no clear evidence for the presence of MeV energy electrons as required for runaway breakdown in the red sprite data.

Future data are needed to clearly identify and quantify the ion emissions either from the A-state in the near infrared or the B-state in the UV. Spectra of the precursor high altitude blue flash ("elve") would be useful in establishing local conditions at the onset of the sprite. Measurements of the electric field and electron densities at the 20 to 40 km altitudes are critical for assessing the onset of sprite-produced chemical reactions. Direct measurements of sprite-produced radiances in the infrared will aid in the assessment of the electron energy distributions in the sprite and the impact on atmospheric chemistry.

Acknowledgments. We acknowledge useful discussions with R.A. Armstrong of MRC. L.G.Piper of PSI provided insight in the spectral analysis. R. Rairden provided assistance in the calibration of the Lockheed data.

References

Anderson, G.P., et al., MODTRAN 2: Suitability for remote sensing, SPIE International Symposium on Optical Engineering and Photonics in Aerospace and Remote Sensing, April 1993.

Armstrong, R.A., private communication, 1995.

Chang, B. and C. Price, Can gamma radiation be produced in the electrical environment above thunderstorms?, *Geophys. Res. Lett.*, *22*, 1117, 1995.

Fraser, M.E., W.T. Rawlins, and S.M. Miller, Infrared (2 to 8 μm) fluorescence of the $W^3\Delta_u \rightarrow B^3\Pi_g$ and $w^1\Delta_u \rightarrow a^1\Pi_g$ systems of nitrogen, *J. Chem. Phys, 88,* 538, 1988.

Green, B.D, et al. LABCEDE fluorescence investigations, *AFGL-TR-88-0186*, 1988 (available upon request).

Hampton, D.L., M.J. Heavner, E.M. Wescott, D.D. Sentman, Optical spectral characteristics of sprites, *Geophys. Res. Lett, 23,* 89, 1996.

Lyons, W.A., Characteristics of luminous structures in the stratosphere above thunderstorms as imaged by low-light video, *Geophys. Res. Lett., 21*, 875, 1994.

Mende, S.B., R.L. Rairden, G.R. Swenson, W.A. Lyons, Sprite spectra; N_2 1PG band identification, *Geophys. Res. Lett., 22*, 2633, 1995.

Milikh, G.M., K. Papadopoulos, and C.L. Chang, On the physics of high altitude lightning, *Geophys. Res. Lett., 22*, 22, 85, 1995.

Pasko, V.P., U.S. Inan, Y.N. Taranenko, and T.F. Bell, Heating, ionization and upward discharges in the mesosphere due to intense quasi-electrostatic thundercloud fields, *Geophys. Res. Lett., 22*, 365, 1995.

Piper, L.G., B.D.Green, W.A.M. Blumberg, S.J. Wolnik, N_2^+ Meinel band quenching, *J. Chem. Phys., 82*, 3139, 1985.

Piper, L.G., K.W. Holtzclaw, B.D. Green, W.A.M. Blumberg, Experimental determination of the Einstein coefficients for the N_2(B-A) transition, *J. Chem. Phys., 90*, 5337, 1989.

Piper, L.G., Energy transfer studies on N_2(X,v) and N_2(B), *J. Chem. Phys., 97*, 270, 1992.

Rawlins, W.T., M.E. Fraser, and S.M. Miller, Rovibrational excitation of nitric oxide in the reaction of O_2 with metastable atomic nitrogen, *J. Chem. Phys., 93*, 1097, 1989.

Sentman, D.D. and E.M. Wescott, Observations of upper atmospheric optical flashes recorded from an aircraft, *Geophys. Res. Lett.,20*, 2857, 1993.

Sentman, D.D. and Westcott, E.M., Red sprites and blue jets: high altitude optical emissions linked to lightning, *EOS 77*, 1, 1996.

Stanton, P.N. and R.M. St. John, Electron excitation of the first positive bands of N_2 and of the first negative and Meinel bands of N_2^+, *J. Optical Soc. Amer.,59*, 252, 1969.

B.D. Green, M.E. Fraser, W.T. Rawlins, Physical Sciences Inc., 20 New England Business Center, Andover, MA (e:green@psicorp.com).

L. Jeong and W.A.M. Blumberg, Phillips Laboratory, Hanscom AFB, MA 01731 (jeong@plh.af.mil)

S.B. Mende, Space Sciences Laboratory, U. California. Berkeley, CA 94720 (mende@ssl.berkeley.edu).

G.R. Swenson , Lockheed Martin Palo Alto Research Lab., 3251 Hanover St., Palo Alto, CA 94304 (swenson@sag.space.lockheed.com).

D.L. Hampton, E.M. Wescott,and D.D. Sentman, Geophysical Institute, 903 Koyukuk Dr. Fairbanks, AK 99775 (dsentmann@guiaf.gi.alaska.edu).

(Received date - Dec. 21, 1995; revised date - June 24, 1996; accepted date - July 2, 1996)